

# **Faraday-active Fabry-Perot Resonator: Transmission, Reflection, and Emissivity**

**Anatoliy Liptuga,<sup>1</sup> Vasyi Morozhenko,<sup>1</sup> Viktor Pipa,<sup>1</sup>  
Evgen Venger<sup>1</sup>, and Theodor Kostiuk,<sup>2,\*</sup>**

<sup>1</sup>*V. Lashkaryov Institute of Semiconductor Physics, 41 Pr. Nauky, Kyiv 03028, Ukraine.*

<sup>2</sup>*NASA Goddard Space Flight Center, Code 693, Greenbelt, MD 20771, USA.*

*\*Corresponding author: theodor.kostiuk@nasa.gov*

The propagation of light within a semiconductor Faraday-active Fabry-Perot resonator (FAFR) is investigated theoretically and experimentally. It is shown that an external magnetic field radically changes the angular and spectral characteristics of transmission, reflection and emissivity of the resonator not only for polarized, but also for unpolarized light. Suppression of interference patterns and phase inversion of the interference extrema were observed in both monochromatic and polychromatic light. The investigations were carried out for the plane-parallel plates of n-InAs in the spectral range of free charge carrier absorption. The results can be used to create new controllable optical and spectroscopic devices for investigation of Faraday-active material properties and for control of parameters of plane-parallel layers and structures.

OCIS codes: 120.2230, 230.3810, 300.6340, 120.7000, 120.5700, 290.6815.

## 1. Introduction.

An interest in the study of methods of control of infrared (IR) radiation with the purpose of creating new optical devices has grown in recent years. For light in the visible and near-infrared range the effects of Kerr and Pockels [1] are used successfully for these purposes. In the middle and far IR spectral region the application of the Faraday effect in optical resonator structures (Fabry-Perot resonators) is promising. Interference effects in such structures set conditions for their selective properties with respect to wavelength, direction of propagation and polarization of light. These effects result in modification of the spectral and angular characteristics of the intensity of transmitted, reflected, and self-emitted (e.g., thermal emission) light.

By applying an external magnetic field to an optical resonator of a magneto-optical medium it is possible to change the conditions of propagation of incident light and to dynamically affect its characteristics.

Although much attention has been given to the investigation of transmission and reflection of magneto-optical single-layered [2-6] and multilayer [6-10] resonator structures, there are a number of questions, which require more careful investigation. This paper is dedicated to the theoretical and experimental investigation of the influence of the magnetic field to angular, spectral and polarization characteristics of transmission, reflection and emissivity of a single-layered Faraday-active Fabry-Perot resonator (FAFR).

The interference effects in the magnetic field are investigated theoretically and tested experimentally both for monochromatic polarized and unpolarized light and for polychromatic light. The theoretical approach presented here is more general than previous work. In contrast to previous work [2-5, 7-10], where the recurrent summing up of multiple reflections was used, the presented theory is based on the method of boundary conditions with the application of  $4 \times 4$

matrices. Unlike the theoretical matrix approach in [6], here the dependence of the dielectric tensor of a magneto-active medium on the applied magnetic field is not limited to linear approximation. This new approach is important for investigating optical parameters of FAFR, based on doped semiconductors.

## 2. Model and theory

Let us consider FAFR as a plane-parallel plate of thickness  $l$  ( $0 \leq z \leq l$ ) placed in a vacuum. A constant magnetic field  $\mathbf{H}$  is perpendicular to the layer and has components  $(0,0,H)$ . The optical properties of the layer are described by the frequency- and the magnetic field dependent dielectric tensor  $\varepsilon(\omega,H)$ , whose components obey the conditions  $\varepsilon_{xx} = \varepsilon_{yy} \neq \varepsilon_{zz}$ ,  $\varepsilon_{xy} = -\varepsilon_{yx}$ , with all other off-diagonal components equal 0.

For the electric field  $\mathbf{E} \propto \exp(i\mathbf{k}\mathbf{r} - i\omega t)$  the wave equation takes the form

$$k_0^2 \mathbf{D} - k^2 \mathbf{E} + \mathbf{k}(\mathbf{k}\mathbf{E}) = 0. \quad (1)$$

Here  $\mathbf{D} = \varepsilon \mathbf{E}$  is the electrical induction,  $\mathbf{k}$  is the wave vector,  $k_0 = \omega/c$ .

Since the  $z$  axis is the axis of axial symmetry, the wave vector can be selected in the form  $\mathbf{k} = (q,0,k_z)$ , where  $q$  is the real projection. For brevity, we will use the dimensionless quantities

$$n_z = k_z/k_0, \quad \xi = q/k_0, \quad s_1 = (1 - \xi^2)^{1/2}, \quad s_2 = (\varepsilon_{zz} - \xi^2)^{1/2}. \quad (2)$$

From the dispersion equation with assigned  $q$  and  $\omega$  we obtain

$$(n_z^\pm)^2 = (2\varepsilon_{zz})^{-1} [2\varepsilon_{xx}\varepsilon_{zz} - \xi^2(\varepsilon_{zz} + \varepsilon_{xx}) \pm f], \quad (3)$$

where  $f = [\xi^4(\varepsilon_{zz} - \varepsilon_{xx})^2 - 4\varepsilon_{xy}^2 s_2^2 \varepsilon_{zz}]^{1/2}$ .

Thus, an electric field in the plate medium is represented by the sum of four plane waves.

Let us represent the amplitude of the wave incident on surface  $z = 0$  at angle  $\vartheta$  as the sum of wave amplitudes with  $s$  and  $p$  polarizations:  $\mathbf{E}_i = \mathbf{E}_{is} + \mathbf{E}_{ip}$  and calculate the coefficients of reflection and transmission for the incident wave for each of the polarizations.

For the wave with  $s$  polarization ( $\mathbf{E}_{is} = (0, -E_i, 0)$ ), the wave amplitudes of the electric field in vacuum ( $z \leq 0$ ) form the components of the 4-vector  $\mathbf{E}_s = (-2s_1 E_i, E_{rx}, 2s_1 E_{ry}, 0)$ , where  $E_{rx}, E_{ry}$  are the projections of the reflected wave amplitude. A projection of the field along the  $x$  axis in the plate takes the form

$$E_x(z) = A_+ \exp(ik_z^+ z) + B_+ \exp(-ik_z^+ z) \\ + A_- \exp(ik_z^- z) + B_- \exp(-ik_z^- z). \quad (4)$$

The  $E_y$  and  $E_z$  components of the electric field in the plate can be expressed as  $E_x$  by using Eq. (1). The amplitudes  $A_{\pm}$  and  $B_{\pm}$  determine the components of the 4-vector  $\mathbf{E}_0 = (A_+, A_-, B_+, B_-)$ .

The tangential components of electrical and the magnetic fields are continuous on the surfaces of the FAFR plate. The boundary conditions on the plane  $z = 0$  give rise to the relationship  $\mathbf{E}_s = M_{1s} \mathbf{E}_0$ , where  $M_{1s}$  is the  $4 \times 4$  transfer matrix. The elements of matrix  $M_{1s}$  (and other matrices that are used in our calculation) are given in the Appendix.

The field  $E_x(l)$  is expressed by the components of the vector  $\mathbf{E}_l = (\tilde{A}_+, \tilde{A}_-, \tilde{B}_+, \tilde{B}_-)$ , where  $\tilde{A}_{\pm} = A_{\pm} \exp(ik_z^{\pm} l)$ ,  $\tilde{B}_{\pm} = B_{\pm} \exp(-ik_z^{\pm} l)$ . The vectors  $\mathbf{E}_l$  and  $\mathbf{E}_0$  are related by the equation  $\mathbf{E}_0 = M_2 \mathbf{E}_l$  where  $M_2$  is the diagonal  $4 \times 4$  propagation matrix; its elements are

$$a_{11} = \exp(-ik_z^+ l), \quad a_{22} = \exp(-ik_z^- l), \quad (5)$$

$$a_{33} = \exp(ik_z^+ l), \quad a_{44} = \exp(ik_z^- l)$$

Using the boundary conditions at  $z = l$ , we obtain the equation  $\mathbf{E}_t = M_3 \mathbf{E}_t$ . Here  $M_3$  -  $4 \times 4$  matrix,  $\mathbf{E}_t = (E_{tx}, E_{ty}, 0, 0)$ , where  $E_{tx}, E_{ty}$  are the field components of the transmitted wave at  $z = l$ . Finally we find that the amplitudes of the light waves in the range  $z \leq 0$  are related to those in the range  $z \geq 0$  by the matrix equation

$$\mathbf{E}_s = C^{-1} S \mathbf{E}_t, \quad (6)$$

where  $C = -2(C_+ - C_-)$ ,  $S = M_{1s} \times M_2 \times M_3$ .

For the incident wave of  $p$  polarization ( $\mathbf{E}_{ip} = (s_1 E_i, 0, -\xi E_i)$ ), we introduce the 4-vector  $\mathbf{E}_p = (2s_1 E_i, 2E_{rx}, E_{ry}, 0)$  and get

$$\mathbf{E}_p = C^{-1} P \mathbf{E}_t, \quad (7)$$

where  $P = M_{1p} \times M_2 \times M_3$ . Here  $M_{1p}$  -  $4 \times 4$  is a matrix with the elements  $n_{ij}$  (see Appendix).

The amplitudes of reflection  $r_{v\alpha} = E_{r\alpha}/E_{iv}$  and transmission  $t_{v\alpha} = E_{t\alpha}/E_{iv}$  ( $\alpha = x, y, z$ ,  $v = s, p$ ) are determined by the elements  $v_{ij}$  of the respective matrices (the elements  $s_{ij}$  of the matrix  $S$  and the elements  $p_{ij}$  of the matrix  $P$ ). The reflection  $R_v$  and transmission  $T_v$  are expressed in the form

$$R_v = \sum_{\alpha} |r_{v\alpha}|^2, \quad T_v = \sum_{\alpha} |t_{v\alpha}|^2. \quad (8)$$

Using the notations  $b_v = -v_{42}/v_{41}$ ,  $d_v = (b_v v_{11} + v_{12})^{-1}$ , we get

$$r_{sx} = -2s_1 (b_s s_{21} + s_{22}) d_s, \quad (9)$$

$$r_{sy} = -(b_s s_{31} + s_{32})d_s, \quad r_{sz} = r_{sx} \tan \vartheta,$$

$$r_{px} = s_1(b_p p_{21} + p_{22})d_p, \quad (10)$$

$$r_{pz} = r_{px} \tan \vartheta.$$

$$T_v = 4|Cd_v|^2(|b_v|^2 + \cos^2 \vartheta). \quad (11)$$

The complete reflection  $R$  and transmission  $T$  for the incident unpolarized wave are expressed in the form

$$R = (R_s + R_p)/2, \quad T = (T_s + T_p)/2. \quad (12)$$

The contributions of  $s$ - and  $p$ -polarized waves to reflected and transmitted unpolarized light are determined by the same expression (Eq. (8)) as corresponding partial components of the reflection  $R_v$  and transmission  $T_v$  for polarized light.

The dependence of the reflection and transmission on the frequency  $\omega$  and the incidence angle  $\vartheta$  determines also the qualitative spectral and angular characteristics of the intensity of self-emitted thermal radiation of a FAFR. According to Kirchhoff's law, the emissivity ( $A$ ) of a FAFR is described by the equation

$$A = 1 - R - T \quad (13)$$

### 3. Theoretical results and discussing.

The theoretical investigations were carried out for the n-InAs plane-parallel plate that was used in our experiments (Fig. 1). Wavelengths used in the calculations correspond to the spectral range of free charge carrier absorption of InAs. The following parameters were used in the

modeling: electron concentration  $N_e = 1.4 \times 10^{18} \text{ cm}^{-3}$ , plate thickness  $l = 0.08 \text{ mm}$ , electron effective mass  $m^* = 0.04m_e$  ( $m_e$  is the electron mass) [11].

For the dielectric tensor  $\varepsilon(\omega, H)$  of the magneto-active medium we used Drude's model, with the scalar at  $H = 0$  RF permittivity  $\varepsilon_\infty = 11.8$ . To take into consideration a dispersion of the absorption coefficient, which was determined from the sample absorption spectra at  $H = 0$ , the dependence of relaxation time  $\tau$  on the wavelength  $\lambda = 2\pi c/\omega$  was  $\tau = 1.3 \times 10^{-11} \lambda^{-1}$  in the calculations (with  $\lambda$  in  $\mu\text{m}$ ).

Figure 2 (a-c) shows the dependence of the angular distribution of the resonator transmission on the magnetic field for the s-polarized ( $T_s(\vartheta)$ ), p-polarized ( $T_p(\vartheta)$ ) and unpolarized ( $T(\vartheta)$ ) light. The change of the magnetic field is shown both in the absolute (right scale) and in relative units  $\chi = (n_z^+ - n_z^-)l\lambda^{-1}$  (left scale). The parameter  $\chi$  characterizes an interaction of the magneto-active medium of the FAFR with light and, as will be seen below, is useful for analyzing the results.

At  $H = 0$  the angular distribution of transmission has a lobe-like character and correspond to a number of resonance maxima (lobes) and minima with the high contrast. When the incidence angle approaches  $90^\circ$ , the transmissions decreases in view of a sharp increase of the reflection from the plate faces (Fig. 3). For the p-polarized light the reflection from the faces is close to zero in region of the Brewster angle ( $\vartheta_B \approx 71.5^\circ$ ). Interference in these conditions is absent and transmission is maximum, independent of the position of the resonance lobe.

In the magnetic field the lobes split into two secondary lobes, which diverge and decrease in amplitude as the field is increasing. When  $\chi = 0.25$  the contrasts of the angular distribution reach a minimum value.

With a further increasing field the secondary lobes begin to merge pairwise with the neighboring one and at  $\chi = 0.5$  the angular distributions of the transmission take a pronounced lobe-like character again. However, there is an inversion of the resonance extrema: positions of the lobes correspond to the minima at  $H = 0$ . Note, that at  $\chi = 0.5$  the transmission of the p-polarized light at  $\vartheta \approx \vartheta_B$  is considerably decreased (see Fig. 2b). This suggests that the transmitted waves interfere in the magnetic field.

It is necessary to note, that the effects of the magnetic field on the transmission of unpolarized light are no less than on polarized light. The changes of  $T(\vartheta)$  in the magnetic field (Fig. 2c) is qualitatively and quantitatively similar to changes of  $T_s(\vartheta)$  (shown in Fig. 2a). The small difference of the contrasts is caused by the difference of the reflection coefficients of the plate faces for unpolarized and for s-polarized light at oblique incidence.

The dependence of the angular distribution of the reflection ( $R_s(\vartheta)$ ,  $R_p(\vartheta)$ ,  $R(\vartheta)$ ) of a FAFR on the magnetic field is shown in Fig. 3. The state of polarization of the incident light corresponds to that in Fig. 2. The angular distributions of reflection at  $H = 0$  have also a contrasting lobe-like character. However, their behavior in the magnetic field differs from that discussed above for transmission distributions. In this case the interference minima split. Maxima lobes appear in their place, with intensity increasing with increasing magnetic field.

When  $\chi = 0.25$ , the amplitudes of the original lobes (at  $H = 0$ ) are almost equal to the amplitude of the appearing ones and the angular distributions of the reflections,  $R_s(\vartheta)$ ,  $R_p(\vartheta)$  and  $R(\vartheta)$ , become practically homogeneous.

At  $\chi = 0.5$  the angular distributions have a lobe-like character again, but with the inversion of the resonance extrema.

$R_p(\vartheta)$  also has a peculiarity in the region of the Brewster angle,  $\vartheta_B \approx 71.5^\circ$  (Fig. 3b). While there was no reflection at  $H = 0$ , at  $H = 42$  kG,  $\chi = 0.5$  the interference lobe is clearly observed. This fact confirms the above conclusion (Fig. 2b) that the magnetic field results in the appearance of interference effects for p-polarized light whose reflection coefficient is equal to zero.

As in the case of transmission, in the presence of a magnetic field introduces changes in the reflection of unpolarized light (Fig. 3c) as well as in reflection of polarized light (Fig. 3a). The effects are qualitatively and quantitatively similar for both transmission and reflection. (see Figs. 3a and 3c).

Since the changes of transmission and reflection of the unpolarized light in the magnetic field are observed also at normal incidence, this effect is not explained by the polarizing action of the plate faces at  $\vartheta \neq 0$ . The cause is a change of the conditions of the multibeam interference in the magnetic field. The magnetic field redistributes the polarization planes of the waves of light inside the resonator. As a result, the interference of the transmitted and reflected waves can be suppressed or phase shifted by a phase difference of  $\pi$ .

Fig. 4 presents the calculated fringes of constant inclination of the transmitted light when FAFR is illuminated by an unpolarized polychromatic  $\lambda = 7.849 - 7.974$   $\mu\text{m}$  source. The calculations

are limited to the first interference order. As is seen, at  $H = 0$  (Fig. 4a) the fringes have a form of contrasting rings, painted in accordance with the wavelength of the interference lobe (the scale of wavelengths is shown on top).

In the magnetic field  $H = 21$  kG (Fig. 4b) the angular dispersion of the resonator disappears. The transmitted light does not have the selected wavelengths (painted by grey) and the FAFR transmission is close to the transmission of a non-resonator.

When  $H = 42$  kG (Fig. 4c) the fringes of constant inclination are clearly visible again. However, their color distribution has changed. In this case the two orders of interference are observed: the truncated blue end first order and the second one when  $\vartheta > 23^\circ$ . Such changes of the angular dispersion are caused by the inversion of the interference extrema in polychromatic light.

In Fig.5 the angular dependence of the FAFR emissivity is shown for  $\lambda = 7.96$   $\mu\text{m}$  at different values of magnetic field. With  $H = 0$  (Fig. 5a) the emissivity has a multi-peaked pattern with a narrow central main lobe and three axially symmetric radially diverging secondary (conical) lobes. The amplitudes of the lobes are dependent on the resonator parameters such as the coefficient of reflection and absorption [12].

In a magnetic field where  $\chi = 0.25$ , the angular dependence supports a greater number of relatively weak minor lobes, making the emission more uniform, making it more like emission from a nonresonant structure (Fig. 5b).

In the field  $H = 42$  kG (Fig. 5c) angular dependence again takes on a clear multi-lobed structure, but with no axially directed maximum emission. The central lobe is missing and the axial emission is minimum. Only flared minor lobes are present. Therefore, the magnetic field

determines the angular distribution of thermal emission and this property of FAFR can be used to generate controlled sources of infrared emission.

It is necessary to emphasize, that the Faraday effect does not appear in natural light, it is present only in polarized light. Effective influence of the magnetic field on the characteristics of the reflection and transmission of unpolarized light is the distinguishing characteristic of the FAFR. This offers possibilities to develop new optical procedures and devices using this property of the Faraday-active Fabry-Perot resonator.

#### 4. Experimental results.

The spectral dependence of transmission and reflection of a FAFR in a magnetic field were measured experimentally. The experimental setup is shown in Fig. 1. For the measurements a plane-parallel semiconductor plate of *n*-InAs with electron concentration  $N_e = 1.4 \cdot 10^{18} \text{ cm}^{-3}$  was used. The plate was cut from a single crystal bar, then ground and subsequently polished on the broad faces. The  $10 \times 5 \text{ mm}^2$  sample had thickness  $l = 0.08 \text{ mm}$ ; the deviation from plane-parallelism was no greater than a few seconds of arc.

The plate was placed between the magnet poles so that the magnetic field was directed normal to the broad faces of the sample. The spectra were recorded by a FTIR with a spectral resolution of  $2 \text{ cm}^{-1}$  in the spectral range of free carriers absorption. The incident light was unpolarized.

Fig. 6 shows the experimental transmission spectra ( $T(\lambda)$ ) of the plane-parallel *n*-InAs plate at  $H = 0$  (dotted line) and at  $H = 24 \text{ kG}$  (solid line) at normal incidence of light. A top scale shows a change of the parameter  $\chi$ , which was calculated for the plate used.

The initial transmission spectrum ( at  $H = 0$  ) is typical for a Fabry-Perot resonator with an interference pattern of alternating maxima and minima. As a result of the absorption dispersion, the contrast of the interference pattern decreases with increasing wavelength.

When  $H = 24$  kG, in the spectral range  $6 < \lambda < 7.5$   $\mu\text{m}$  the decrease of the interference pattern contrast caused by the splitting of the maxima into two secondary peaks is clearly visible.

In the  $\lambda \approx 7.5$   $\mu\text{m}$  region (  $\chi \approx 0.25$  ), where the secondary maxima are equally-spaced, double the number of low-contrast  $T(\lambda)$  maxima is observed. A link is observed in the interference pattern.

With a further increasing  $\lambda$  the secondary paired lines merge and the contrast grows, however, the phase of the interference extrema is inverted relative to the  $H=0$  case.

Shown in Fig. 7 are the experimental reflection spectra (  $R(\lambda)$  ) at  $H = 0$  (dotted line) and  $H = 24$  kG (solid lines). Reflection was registered near the Brewster angle  $\vartheta = (71.5 \pm 1)^\circ$ .

For the unpolarized incident light (Fig. 7a) in the field  $H = 24$  kG the interference pattern is suppressed and even disappears in the  $\lambda = 9.5 - 10.5$   $\mu\text{m}$  region. Notice that in this case the minimum link appears at  $\chi \approx 0.5$ . When advancing to the red region ( $0.5 < \chi < 1$ ) the interference appears again, but the inversion of interference extrema is not observed. Theoretical analysis shows, the disappearance of the link at  $\chi \approx 0.25$  (as seen in Fig. 6) is caused by the fact that at the incidence angles  $\vartheta > \vartheta_B$  there is no phase jump  $\pi$  at the reflection of light from the interface of the semiconductor/air.

Fig. 7b shows the reflection spectrum of a p-polarized component of the incident light (  $R_p(\lambda)$  ).

The reflection of p-polarized light is absent at the Brewster angle. But, in the magnetic field the

appearance of the reflected light with the presence of interference is observed. In a range  $\lambda = 10 - 10.7 \mu\text{m}$  the interference disappears and appears again at  $\lambda > 10.7 \mu\text{m}$ .

Unfortunately, the absorption dispersion degrades the cavity Q factor and strongly distorts the dependence of  $R_p(\lambda)$ . In order to illustrate this the  $R_p(\lambda)$  dependence on  $\lambda$  was calculated in the absence of absorption (presented on Fig. 7c). As is seen, in this case  $R_p(\lambda)$  has a bell-shaped form with a smooth top at  $\lambda \approx 10.2 \mu\text{m}$  and the contrast interference on the wings. This form of  $R_p(\lambda)$  is explained by the rotation of the polarization plane of the light when it passes the resonator volume. When the light has reached the back face, it contains the s- and p-components. The s- component reflects and undergoes rotation again. As a result, the p-polarized coherent waves appear in the reflection light. They define both the average value of reflection and the contrast of the interference pattern. At  $\chi = 0.5$  only one such wave is presents and the multibeam interference is absent.

It is important to note, that the parameter  $\chi$  used for the analysis includes the concentration and the effective mass of the electrons,  $\epsilon_\infty$ , thickness and other parameters of the *n*-InAs plate. Thus, registration and analysis of the reflection and transmission in the magnetic field can be an effective method of investigating and monitoring of plane-parallel layers and structures. In this case, unlike the known magneto-optical phenomena, unpolarized light can be used, which simplifies the method. In addition, the analysis of the interference pattern is more convenient and simpler than the analysis of the polarization peculiarities of the transmitted (reflected) light.

The effects of a magnetic field on thermal emission spectra of FAFR was experimentally investigated and discussed by the authors in previous publications [13, 14]. Therefore, we do not discuss these results in detail here. We do note that calculations of spectral and angular

dependence and character of the thermal emission using Eq. 13 agree well with experimental and theoretical results in our earlier investigations

### **Conclusions.**

In summary, theoretical and experimental investigations of reflection and transmission of a Faraday-active Fabry-Perot resonator in the magnetic field were carried out. The presented theory makes it possible to calculate the parameters of a resonator for an arbitrary incidence angle of light. Since the theory is not magnetic field restricted to a linear approximation, it can be used for semiconductor layers and structures in the range of free current carriers absorption.

It is established that under the conditions of multibeam interference the magnetic field substantially changes the characteristics of the transmission and reflection of both unpolarized and polarized light. It is shown that these effects appear also for the polychromatic light. These results are new and nontrivial, since only polarized monochromatic light is used in describing all classical magneto-optical effects.

Obtained results can be used for developing new magneto-optical devices, such as as controlled dispersion elements, dynamic infrared imitators, and other devices with adjustable reflection/transmission and others, which can work both with the polarized and natural light.

The possibility of theoretical analysis of interference patterns of FAFR structures makes it possible to develop new procedures for determining parameters of solids and plane-parallel plates, layers and structures.

## References

1. M. Bass (editor in chief), J.M. Enoch , C.M. DeCusatis, V. Lakshminarayanan, G. Li, C. MacDonald, V.N. Mahajan and E. Van Stryland, *Handbook of Optics*, Vol. V: *Atmospheric Optics, Modulators, Fiber Optics, X-Ray and Neutron Optics* (3-rd edition, Mc/Graw-Hill, New York, Chicago, San Francisco, Lisbon, London, Madrid, Mexico City, Milan, New Delhi, San Juan, Seoul, Singapore, Sydney, Toronto, 2009)
2. R.Rosenberg, C.B.Rubinstein, and D.R.Herriott, "Resonant optical Faraday rotation." *Appl. Optics* **3**, 1079-1083 (1964).
3. V.A.Shamburov and E.A.Evdishchenko, "Exact Jones matrix for the plate from the natural gyrotropic nonmagnetic crystal," *Kristallografiya* **38**, 847-849 (1991).
4. H.Y.Ling, "Theoretical investigation of transmission through a Faraday-active Fabry-Perot etalon," *J. Opt. Soc. Am. A*, **11** 754-758 (1994).
5. D.Jacob, M.Vallet, F.Bretenaker, A.Le Floch, and R.Le Naur, "Small Faraday rotation measurement with a Fabry-Perot cavity." *Appl. Phys. Lett.* **66**, 3546-3548 (1995).
6. D.W. Berreman, "Optics in stratified and anisotropic media: 4x4-matrices formulation," *J. Opt. Soc. Am.* **62**, 502-510 (1972).
7. O.V. Ivanov and D.I. Sementsov " Coherent and incoherent reflection and transmission of light in anisotropic layer structures," *Crystallogr. Rep.* **45**, 827-832 (2000).
8. I.V. Semchenko and V.E.Kaganovich, " Selective optical properties of a multilayered periodic gyrotropic structure at an arbitrary angle of incidence of waves," *Crystallogr. Rep.* **49**, 1032-1037 (2004).

9. D.G. Makarov, V.V. Danilov, and V.F.Kovalenko, "Multilayer structures with magnetically controlled light transmission," *Tech. Phys.* **49**, 598-602 (2004)
10. S. N. Kurilkina and A. L. Zykov, "Enhancement of the Faraday effect in finite three-layer periodic media," *Opt. Spectrosc.* **98**, 624-627 (2005).
11. O. Madelung *O Semiconductors: Data Handbook*, (Springer-Verlag, Berlin 2004).
12. K.Yu. Guga, O.G. Kollyukh, A. I. Liptuga, V. Morozhenko and V. I. Pipa, " Features of thermal radiation of plane-parallel semiconductor wafers", *Semiconductors*, **38**, 507-511 (2004).
13. O.G. Kollyukh, A. I. Liptuga, V. Morozhenko and V. I. Pipa, "Magnetic-field modulation of the spectrum of coherent thermal radiation of semiconductor layers," *Phys. Rev.B* **71**, 073306-1 - 073306-4 (2005).
14. O.G. Kollyukh and V. Morozhenko, "Angular and spectral peculiarities of coherent thermal radiation of the magneto-optical Fabry-Perot resonator in magnetic field," *J. Opt. A* **11**, 085503-1 - 085503-6 (2009).

**Appendix.**

The elements of  $M_1$ :

$$m_{11} = C_+(s_1 + n_z^+), \quad m_{12} = C_-(s_1 + n_z^-),$$

$$m_{13} = C_+(s_1 - n_z^+), \quad m_{14} = C_-(s_1 - n_z^-),$$

$$m_{21} = m_{22} = m_{23} = m_{24} = 1,$$

$$m_{31} = m_{13}, \quad m_{32} = m_{14}, \quad m_{33} = m_{11}, \quad m_{34} = m_{12}$$

$$m_{41} = s_2^2 + s_1 \varepsilon_{ZZ} n_z^+, \quad m_{42} = s_2^2 + s_1 \varepsilon_{ZZ} n_z^-,$$

$$m_{43} = s_2^2 - s_1 \varepsilon_{ZZ} n_z^+, \quad m_{44} = s_2^2 - s_1 \varepsilon_{ZZ} n_z^-,$$

where  $C_{\pm} = \varepsilon_{xy}(\varepsilon_{xx} - \xi^2 - n_z^{\pm})^{-1}$ .

The elements of  $M_3$ :

$$c_{11} = C_-(n_z^+ + V)/n_z^+, \quad c_{12} = -(s_1 + n_z^+)/n_z^+, \quad c_{13} = c_{14} = 0,$$

$$c_{21} = -C_+(n_z^- + V)/n_z^-, \quad c_{22} = (s_1 + n_z^-)/n_z^-, \quad c_{23} = c_{24} = 0,$$

$$c_{31} = C_-(n_z^+ - V)/n_z^+, \quad c_{32} = (s_1 - n_z^+)/n_z^+, \quad c_{33} = c_{34} = 0,$$

$$c_{41} = -C_+(n_z^- - V)/n_z^-, \quad c_{42} = -(s_1 - n_z^-)/n_z^-, \quad c_{43} = c_{44} = 0.$$

Here  $V = s_2^2/s_1 \varepsilon_{ZZ}$ .

The elements of  $M_{1p}$ :

$$n_{11} = m_{41}/s_2^2, \quad n_{12} = m_{42}/s_2^2, \quad n_{13} = m_{43}/s_2^2, \quad n_{14} = m_{44}/s_2^2,$$

$$n_{21} = m_{43}/s_2^2, \quad n_{22} = m_{44}/s_2^2, \quad n_{23} = m_{41}/s_2^2, \quad n_{24} = m_{42}/s_2^2,$$

$$n_{31} = C_+, \quad n_{32} = C_-, \quad n_{33} = C_+, \quad n_{34} = C_-,$$

$$n_{41} = m_{11}, \quad n_{42} = m_{12}, \quad n_{43} = m_{13}, \quad n_{44} = m_{14}.$$

Liptuga *et al.* JOSA A

Seven (7) Figures

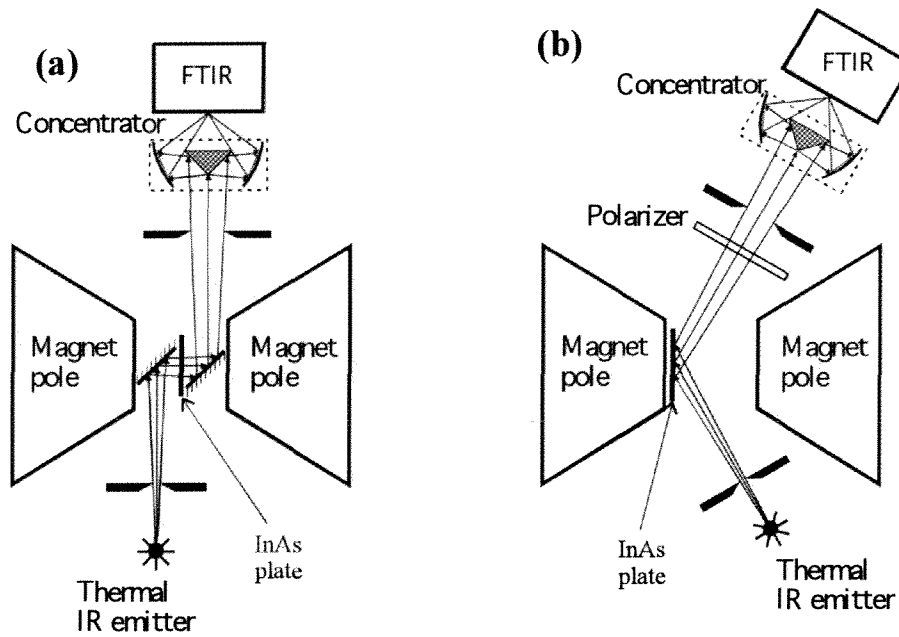


Fig 1. Experimental setup for investigating (a) transmission and (b) reflection of a plane-parallel n-InAs plate in a magnetic field. The Fourier transform interferometer (FTIR) measures the resultant spectrum. The theoretical analysis is also for this FAIR – magnetic field arrangement.

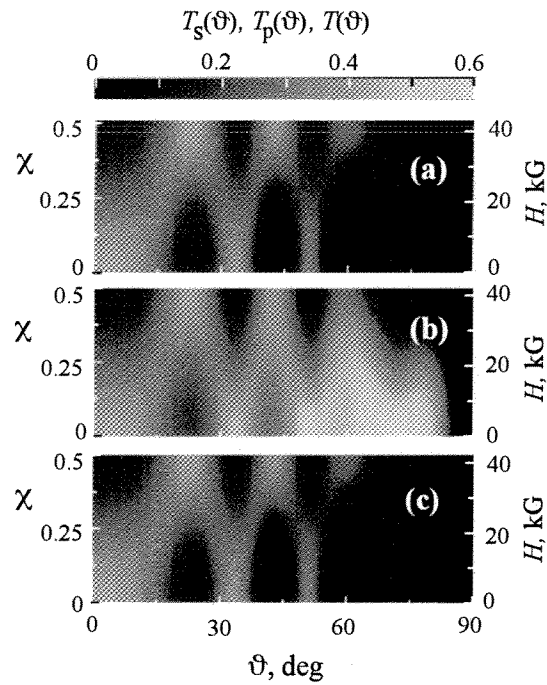


Fig. 2. (Color online) Contour plots of the dependence of the angular distribution of the FAFR transmission on magnetic field. Incident light is: (a) s-polarized; (b) p-polarized; (c) unpolarized.  $\lambda = 7.96 \mu\text{m}$ . In a magnetic field the interference maxima split into doublets, which change their position with increasing  $H$ . They combine with neighboring maxima into a phase reversed single maxima. This effect exists in polarized as well as unpolarized light.

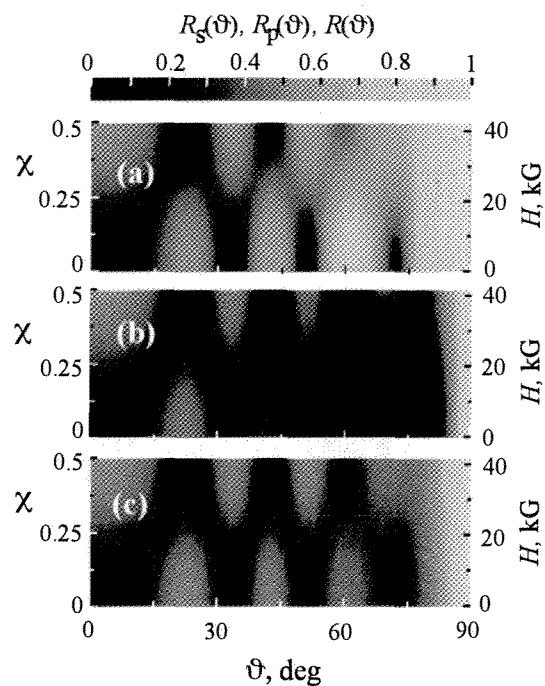


Fig.3. (Color online) Contour plots of the dependence of the angular distribution of the FAFR reflection on magnetic field. Incident light is: (a) s-polarized; (b) p-polarized; (c) unpolarized.  $\lambda = 7.96 \mu\text{m}$ . In a magnetic field the interference minima split into doublets, which change their position with increasing  $H$ . They combine with neighboring minima into phase reversed single minima. This effect exists in polarized as well as unpolarized light.

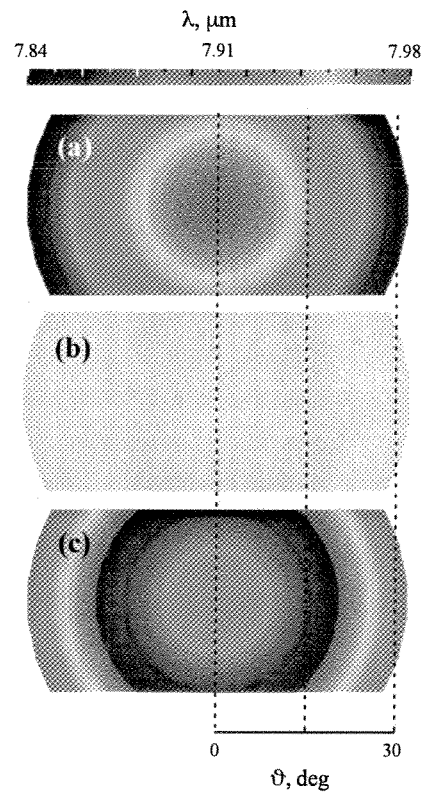


Fig.4. Fringes of constant inclination of the FAFR for an n-InAs resonator of thickness  $l=0.08$  mm. The incident light is unpolarized.  $\lambda = 7.849 - 7.974$   $\mu\text{m}$ . (a)  $H = 0$ ; (b)  $H = 21$  kG; (c)  $H = 42$  kG. The wavelength scale is shown on top. The magnetic field changes the dispersion characteristics of the resonator. Near  $H = 21$  kG the resonator ceases to be a dispersive element and no fringe pattern is observed.

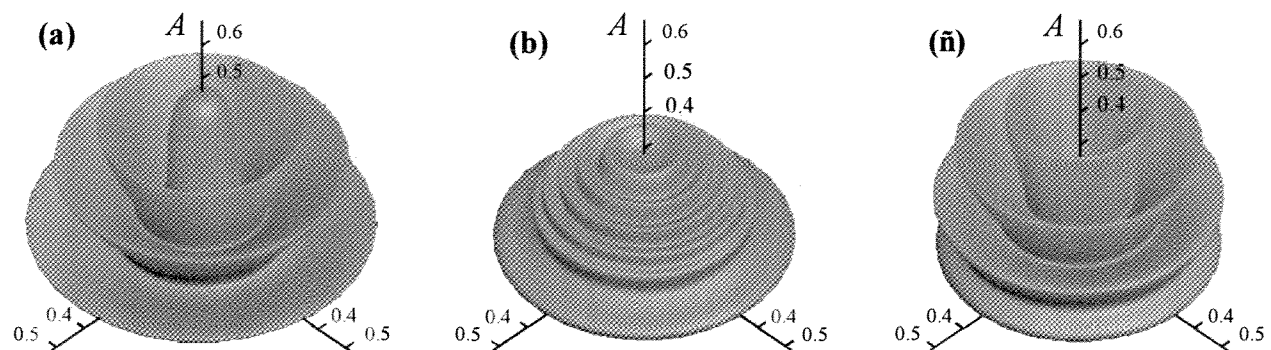


Fig.5. (Color online) Angular dependencies of the FAFR emissivity in magnetic field.  $\lambda = 7.96$   $\mu\text{m}$ . (a)  $H = 0$ ; (b)  $H = 21$  kG,  $\chi = 0.25$ ; (c)  $H = 42$  kG,  $\chi = 0.5$ . Angular dependence of the emissivity changes with the magnetic field, thus, changing the directional pattern of the FAFR thermal emission.

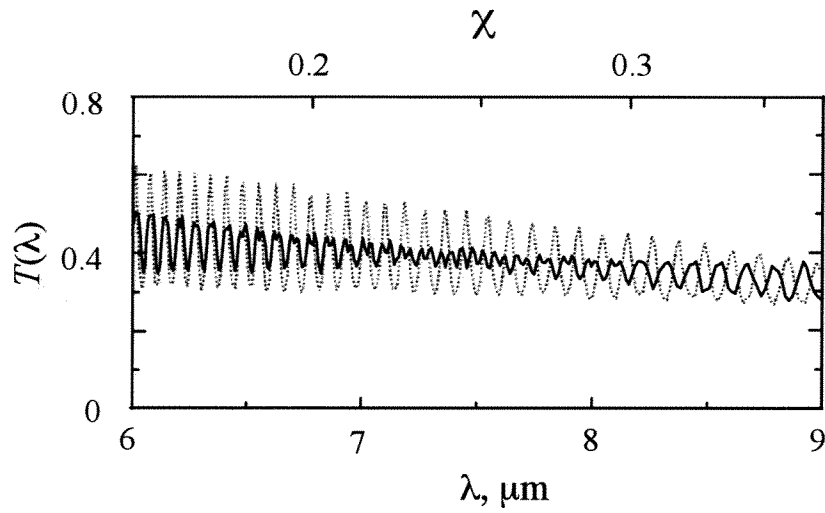


Fig.6. Experimental transmission spectra of the plane-parallel  $n$ -InAs plate at  $H = 0$  (dotted line) and  $H = 24$  kG (solid line) at a normal incidence of light. The incident light is unpolarized. As  $\lambda$  increases interference maxima split, initially minimizing intensity contrast and then combining to form maxima of inverted phase.

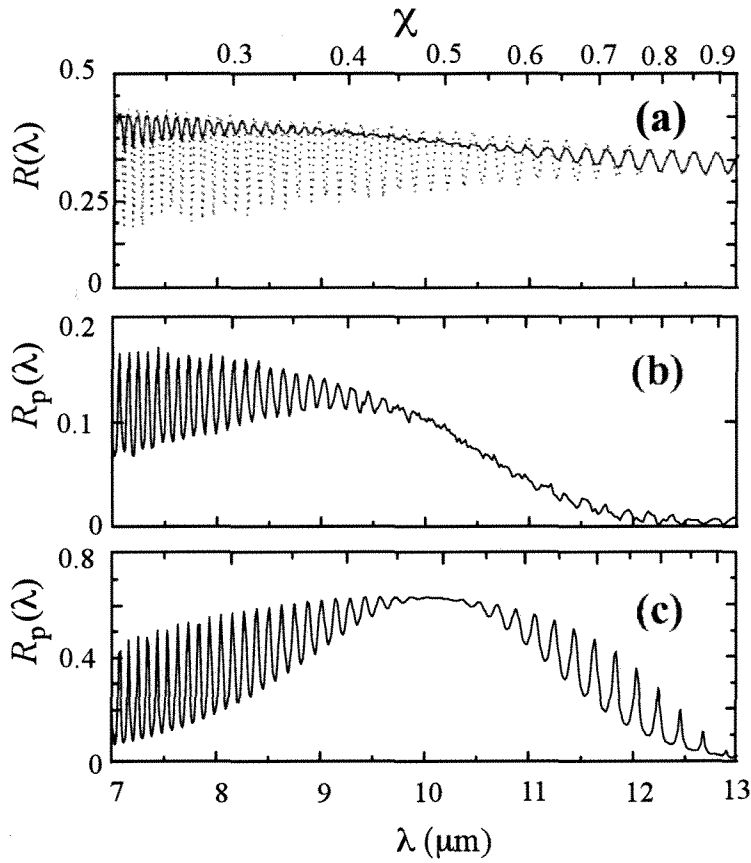


Fig.7. Experimental reflection spectra of the plane-parallel  $n$ -InAs plate at  $H = 0$  (dotted line) and  $H = 24$  kG (solid line). The incidence angle is near the Brewster angle  $\vartheta_1 = (71.5 \pm 1)^\circ$ . The incident light is: (a) unpolarized; (b) p-polarized. Fig. 7c is theoretical reflection spectrum of the p-polarized light in the absence of absorption. (a) In a magnetic field, unpolarized light shows a change in interference contrast with increasing  $\lambda$ . For p-polarized light at Brewster angle incidence the magnetic field leads to the appearance of reflection as well as to interference of the reflected waves ( (b), (c) ).